An HEVI time-splitting discontinuous Galerkin scheme for non-hydrostatic atmospheric modeling[1]

Lei Bao
Department Of Applied Mathematics, University of Colorado at Boulder
Ram Nair, Robert Klöfkorn
National Center for Atmospheric Research(NCAR), Boulder, CO

PDE on the sphere, Boulder, CO
April 7th, 2014

University of Colorado Boulder

NCAR

[1] Manuscript submitted to *Monthly Weather Review*

Outline

Outline

Motivation

1. Peta-scale Super Computing Resources.
2. Atmospheric Model in Non-Hydrostatic Regime.
3. Requirements for discretization methods
    - Existing methods have serious limitations to satisfy all of the following properties:
        1. Local and global conservation
        2. High-order accuracy
        3. Computational efficiency
        4. Geometric flexibility ("Local" method, AMR)
        5. Non-oscillatory advection (monotonic, positivity preservation)
        6. High parallel efficiency (Petascale capability)
    - Discontinuous Galerkin Method (DGM) is a potential candidate
4. Efficient Time Integration Scheme Greatly Needed.
    - **HEVI**-horizontally explicit and vertically implicit is a good option.

Outline

Idealized Non-Hydrostatic Atmospheric Model:

- Based on conservation of momentum, mass and potential temperature (without Coriolis effect) the classical compressible 2D Euler system can be written in vector form:

$$
\begin{aligned}
\frac{\partial \rho}{\partial t} + \nabla \cdot (\rho \mathbf{u}) &= 0 \\
\frac{\partial \rho \mathbf{u}}{\partial t} + \nabla \cdot (\rho\, \mathbf{u} \otimes \mathbf{u} + p\, \mathbf{I}) &= -\rho g\, \mathbf{k} \\
\frac{\partial \rho \theta}{\partial t} + \nabla \cdot (\rho \theta\, \mathbf{u}) &= 0
\end{aligned}
$$

Idealized Non-Hydrostatic Atmospheric Model:

- Based on conservation of momentum, mass and potential temperature (without Coriolis effect) the classical compressible 2D Euler system can be written in vector form:

$$\begin{aligned} \frac{\partial \rho}{\partial t} + \nabla \cdot (\rho \mathbf{u}) &= 0 \\ \frac{\partial \rho \mathbf{u}}{\partial t} + \nabla \cdot (\rho\, \mathbf{u} \otimes \mathbf{u} + p\mathbf{I}) &= -\rho g \mathbf{k} \\ \frac{\partial \rho \theta}{\partial t} + \nabla \cdot (\rho \theta \mathbf{u}) &= 0 \end{aligned}$$

- Removal of hydrostatic balanced state.

$$\frac{d\overline{p}}{dz} = -\overline{\rho} g$$

Terrain-Following z-Coordinates[2]

Physical Grid (x, z) Computational Grid (x, ζ)

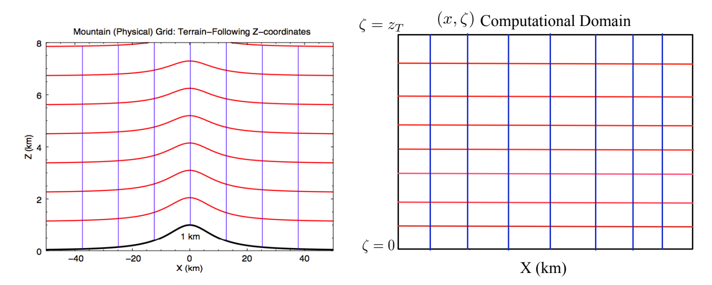

[2] Gal-Chen & Somerville, JCP (1975)

Terrain-Following z-Coordinates[2]

Physical Grid (x,z) Computational Grid (x,ζ)

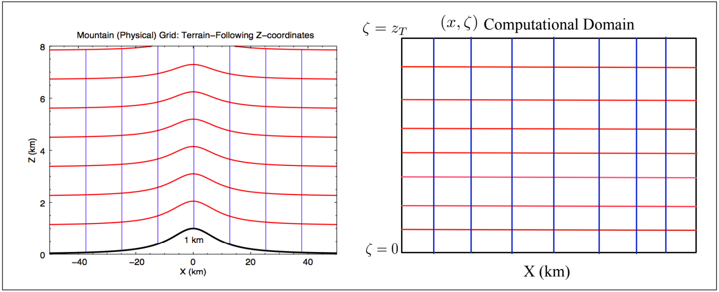

- (x,ζ) coordinates.

$$\zeta = z_T \frac{z-h}{z_T-h}, \quad z(\zeta) = h(x) + \zeta \frac{(z_T-h)}{z_T}; \quad h(x) \le z \le z_T$$

- The metric terms (Jacobians) and new vertical velocity $\tilde{w}$ are

$$\sqrt{G} = \frac{dz}{d\zeta}, G^{ij} = \begin{bmatrix} 0 & \frac{d\zeta}{dx} \\ 0 & 0 \end{bmatrix}; \quad \tilde{w} = \frac{d\zeta}{dt} = \frac{1}{\sqrt{G}}(w + \sqrt{G}G^{12}u)$$

[2] Gal-Chen & Somerville, JCP (1975)

Terrain-Following z-Coordinates [2D Euler System]

- In the transformed (x,ζ) coordinates, the Euler 2D system becomes[3]:

$$\frac{\partial}{\partial t}\begin{bmatrix}\sqrt{G}\rho' \\ \sqrt{G}\rho u \\ \sqrt{G}\rho w \\ \sqrt{G}(\rho\theta)'\end{bmatrix}+\frac{\partial}{\partial x}\begin{bmatrix}\sqrt{G}\rho u \\ \sqrt{G}(\rho u^2+p') \\ \sqrt{G}\rho u w \\ \sqrt{G}\rho u\theta\end{bmatrix}+\frac{\partial}{\partial \zeta}\begin{bmatrix}\sqrt{G}\rho\tilde{w} \\ \sqrt{G}(\rho u\tilde{w}+G^{12}p') \\ \sqrt{G}\rho w\tilde{w}+p' \\ \sqrt{G}\rho\tilde{w}\theta\end{bmatrix}=\begin{bmatrix}0 \\ 0 \\ -\sqrt{G}\rho' g \\ 0\end{bmatrix}.$$

[3] Skamarock & Klemp (2008), Giraldo & Restelli, JCP (2008)

[4] Norman et al., JCP (2010)

[5] Schär (2002), Klemp (2011)

Terrain-Following z-Coordinates [2D Euler System]

- In the transformed (x, ζ) coordinates, the Euler 2D system becomes[3]:

$$\frac{\partial}{\partial t}\begin{bmatrix} \sqrt{G}\rho' \\ \sqrt{G}\rho u \\ \sqrt{G}\rho w \\ \sqrt{G}(\rho\theta)' \end{bmatrix} + \frac{\partial}{\partial x}\begin{bmatrix} \sqrt{G}\rho u \\ \sqrt{G}(\rho u^2 + p') \\ \sqrt{G}\rho uw \\ \sqrt{G}\rho u\theta \end{bmatrix} + \frac{\partial}{\partial \zeta}\begin{bmatrix} \sqrt{G}\rho\tilde{w} \\ \sqrt{G}(\rho u\tilde{w} + G^{12}p') \\ \sqrt{G}\rho w\tilde{w} + p' \\ \sqrt{G}\rho\tilde{w}\theta \end{bmatrix} = \begin{bmatrix} 0 \\ 0 \\ -\sqrt{G}\rho' g \\ 0 \end{bmatrix}.$$

- In Cartesian Coordinates (no orography)($\sqrt{G} = 1, G^{12} = 1; \tilde{w} = w$)[4]:

$$\frac{\partial}{\partial t}\begin{bmatrix} \rho' \\ \rho u \\ \rho w \\ (\rho\theta)' \end{bmatrix} + \frac{\partial}{\partial x}\begin{bmatrix} \rho u \\ \rho u^2 + p' \\ \rho uw \\ \rho u\theta \end{bmatrix} + \frac{\partial}{\partial z}\begin{bmatrix} \rho w \\ \rho wu \\ \rho w^2 + p' \\ \rho w\theta \end{bmatrix} = \begin{bmatrix} 0 \\ 0 \\ -\rho' g \\ 0 \end{bmatrix}.$$

[3] Skamarock & Klemp (2008), Giraldo & Restelli, JCP (2008)

[4] Norman et al., JCP (2010)

[5] Schär (2002), Klemp (2011)

Terrain-Following z-Coordinates [2D Euler System]

- In the transformed (x, ζ) coordinates, the Euler 2D system becomes[3]:

$$\frac{\partial}{\partial t}\begin{bmatrix} \sqrt{G}\rho' \\ \sqrt{G}\rho u \\ \sqrt{G}\rho w \\ \sqrt{G}(\rho\theta)' \end{bmatrix} + \frac{\partial}{\partial x}\begin{bmatrix} \sqrt{G}\rho u \\ \sqrt{G}(\rho u^2 + p') \\ \sqrt{G}\rho uw \\ \sqrt{G}\rho u\theta \end{bmatrix} + \frac{\partial}{\partial \zeta}\begin{bmatrix} \sqrt{G}\rho\tilde{w} \\ \sqrt{G}(\rho u\tilde{w} + G^{12}p') \\ \sqrt{G}\rho w\tilde{w} + p' \\ \sqrt{G}\rho\tilde{w}\theta \end{bmatrix} = \begin{bmatrix} 0 \\ 0 \\ -\sqrt{G}\rho' g \\ 0 \end{bmatrix}.$$

- In Cartesian Coordinates (no orography)($\sqrt{G} = 1, G^{12} = 1; \tilde{w} = w$)[4]:

$$\frac{\partial}{\partial t}\begin{bmatrix} \rho' \\ \rho u \\ \rho w \\ (\rho\theta)' \end{bmatrix} + \frac{\partial}{\partial x}\begin{bmatrix} \rho u \\ \rho u^2 + p' \\ \rho uw \\ \rho u\theta \end{bmatrix} + \frac{\partial}{\partial z}\begin{bmatrix} \rho w \\ \rho wu \\ \rho w^2 + p' \\ \rho w\theta \end{bmatrix} = \begin{bmatrix} 0 \\ 0 \\ -\rho' g \\ 0 \end{bmatrix}.$$

- Alternative formulations are also possible [5] for ζ, but the system of equations remains in flux-from.

$$\frac{\partial \mathbf{U}}{\partial t} + \nabla \cdot \mathbf{F}(\mathbf{U}) = \mathbf{S}(\mathbf{U})$$

where $\mathbf{U} = [\sqrt{G}\rho', \sqrt{G}\rho u, \sqrt{G}\rho w, \sqrt{G}(\rho\theta)']^T$

[3] Skamarock & Klemp (2008), Giraldo & Restelli, JCP (2008)

[4] Norman et al., JCP (2010)

[5] Schär (2002), Klemp (2011)

Outline

Discontinuous Galerkin(DG) Components

Consider a generic form of Euler's System in two dimension.

$$\frac{\partial U}{\partial t} + \nabla \cdot \mathbf{F}(U) = \mathbf{S}(U), \quad \text{in} \quad D \times (0, t_T); \forall (x,y) \in D$$

where $U = U(x,y,t)$, $\nabla \equiv (\partial/\partial x, \partial/\partial y)$, $\mathbf{F} = (F_1, F_2)$ is the flux function.

Discontinuous Galerkin(DG) Components

Consider a generic form of Euler's System in two dimension.

$$\frac{\partial U}{\partial t} + \nabla \cdot \mathbf{F}(U) = \mathbf{S}(U), \quad \text{in} \quad D \times (0, t_T); \forall (x,y) \in D$$

where $U = U(x,y,t)$, $\nabla \equiv (\partial/\partial x, \partial/\partial y)$, $\mathbf{F} = (F_1, F_2)$ is the flux function.

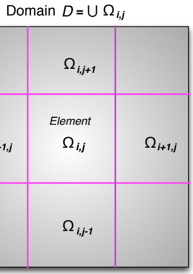

Discontinuous Galerkin(DG) Components

Consider a generic form of Euler's System in two dimension.

$$\frac{\partial U}{\partial t} + \nabla \cdot \mathbf{F}(U) = \mathbf{S}(U), \quad \text{in} \quad D \times (0, t_T); \forall (x,y) \in D$$

where $U = U(x,y,t)$, $\nabla \equiv (\partial/\partial x, \partial/\partial y)$, $\mathbf{F} = (F_1, F_2)$ is the flux function.

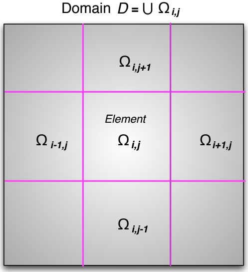

- Weak Galerkin formulation:

$$\frac{\partial}{\partial t}\int_{I_{i,j}} U_h\, \varphi_h\, ds - \int_{I_{i,j}} \mathbf{F}(U_h) \cdot \nabla \varphi_h\, ds \quad + \int_{\partial I_{i,j}} \mathbf{F}(U_h) \cdot \vec{n}\, \varphi_h\, d\Gamma = \int_{I_{i,j}} S_h\, \varphi_h\, ds$$

Discontinuous Galerkin(DG) Components

Consider a generic form of Euler's System in two dimension.

$$\frac{\partial U}{\partial t} + \nabla \cdot \mathbf{F}(U) = \mathbf{S}(U), \quad \text{in} \quad D \times (0, t_T); \forall (x,y) \in D$$

where $U = U(x,y,t)$, $\nabla \equiv (\partial/\partial x, \partial/\partial y)$, $\mathbf{F} = (F_1, F_2)$ is the flux function.

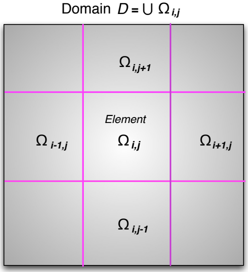

- Weak Galerkin formulation:

$$\frac{\partial}{\partial t} \int_{I_{i,j}} U_h \varphi_h \, ds - \int_{I_{i,j}} \mathbf{F}(U_h) \cdot \nabla \varphi_h \, ds \quad + \int_{\partial I_{i,j}} \hat{\mathbf{F}}(U_h) \cdot \vec{n} \, \varphi_h \, d\Gamma = \int_{I_{i,j}} S_h \, \varphi_h \, ds$$

High-Order Nodal Spatial Discretization

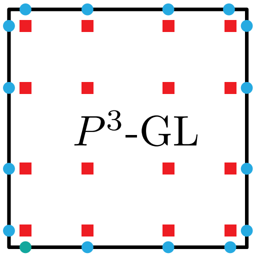

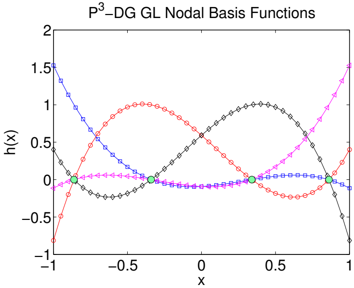

High-Order Nodal Spatial Discretization

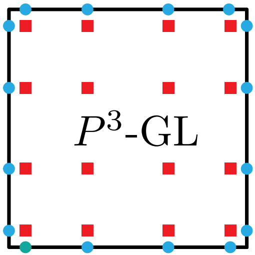

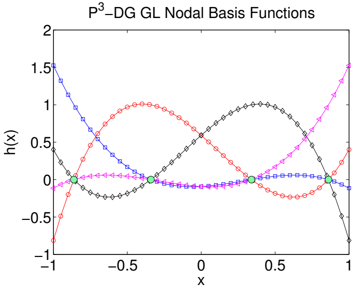

- The resulting form of DG-NH model is a system of ODEs.

$$\frac{dU_h}{dt} = L(U^h), \quad t \in (0, t_T)$$

Outline

Challenges for ODE system

Options & Challenges

- Explicit time integration efficient and easy to implement.
  Stringent CFL constraint $\Rightarrow$ tiny Δt, limited practical value.

$$\frac{C\Delta t}{\bar{h}} < \frac{1}{2N+1}$$

1. Strong Stability-Preserving (SSP)-RK.

Heun's method (2-stage 2$^{\text{nd}}$ order)

$$\begin{array}{c|cc} 0 & 0 & \\ 1 & 1 & 0 \\ \hline & \frac{1}{2} & \frac{1}{2} \end{array}$$

Explicit Runge-Kutta (SSP-RK3) (3-stage 3$^{\text{rd}}$ order)

$$\begin{array}{c|ccc} 0 & 0 & & \\ 1 & 1 & 0 & \\ \frac{1}{2} & \frac{1}{4} & \frac{1}{4} & 0 \\ \hline & \frac{1}{6} & \frac{1}{6} & \frac{2}{3} \end{array}$$

Challenges for ODE system

Options & Challenges

- Explicit time integration efficient and easy to implement.
  Stringent CFL constraint $\Rightarrow$ tiny Δt, limited practical value.

$$\frac{C\Delta t}{\bar{h}} < \frac{1}{2N+1}$$

- Implicit time integration, unconditionally stable but generally expensive to solve. **Overall efficiency still questionable**.

Challenges for ODE system

Options & Challenges

- Explicit time integration efficient and easy to implement.
  Stringent CFL constraint $\Rightarrow$ tiny Δt, limited practical value.

$$\frac{C\Delta t}{\bar{h}} < \frac{1}{2N+1}$$

- Implicit time integration, unconditionally stable but generally expensive to solve. **Overall efficiency still questionable**.
- Semi-implicit time integration
  - Implicit solver for linear part and explicit solver for nonlinear parts. Needs **smart Helmholtz solver**.
  - **HEVI**: horizontally explicit and vertically implicit.

DG-NH Time Stepping-HEVI

For the resulting ODE system

$$\frac{dU_h}{dt} = L(U^h), \text{ with } \frac{C\Delta t}{\bar{h}} < \frac{1}{2N+1}$$

To overcome $\bar{h} = \min\{\Delta x, \Delta z\}$, treat the vertical time discretization (z-direction) in an implicit manner.

- **Benefit**: The effective Courant number is only limited by the minimum horizontal grid-spacing $\min\{\Delta x, \Delta y\}$.
- **Bonus**: The 'HEVI' split approach might retain the parallel efficiency of HOMME for NH equations too.
- Horizontal part and vertical part connected by **Strang-type** time splitting, permitting $\mathscr{O}(\Delta t^2)$ accuracy.
- **Remarks of HEVI**.
  - Particularly useful for 3D NH modeling ($\Delta z : \Delta x = 1 : 1000$).
  - Global NH models adopt the HEVI philosophy, NICAM[6], MPAS[7] etc.
  - Recent high-order FV-NH[8] models based on operator-split method.

[6] Satoh et al. 2008

[7] Skamarock et al. 2012

[8] Norman et al. (JCP, 2011), Ulrich et al. (MWR, 2012)

DG-NH Time Stepping-HEVI

- The Euler system for $\mathbf{U} = (\sqrt{G}\rho', \sqrt{G}\rho u, \sqrt{G}\rho\tilde{w}, \sqrt{G}(\rho\theta)')^T$ is split into horizontal (x) and vertical (ζ or z) components:

$$\begin{aligned}
&\text{(Euler sys)} & \frac{\partial \mathbf{U}}{\partial t} + \frac{\mathbf{F}_x(\mathbf{U})}{\partial x} + \frac{\mathbf{F}_z(\mathbf{U})}{\partial z} &= \mathbf{S}(\mathbf{U}) \\
&(H\text{-part}) & \frac{\partial \mathbf{U}}{\partial t} + \frac{\mathbf{F}_x(\mathbf{U})}{\partial x} &= \mathbf{S}^x(\mathbf{U}) = (0,0,0,0)^T \quad (1) \\
&(V\text{-part}) & \frac{\partial \mathbf{U}}{\partial t} + \frac{\mathbf{F}_z(\mathbf{U})}{\partial z} &= \mathbf{S}^z(\mathbf{U}) = (0,0,-\rho' g,0)^T \quad (2)
\end{aligned}$$

- One possible option is to perform "$H - V - H$" sequence of operations:
  - Advance H-part by $\Delta t/2$ to get $\mathbf{U}^*$, from the initial value $\mathbf{U}^n$
  - Evolve V-part by a full time-step Δt, to obtain $\mathbf{U}^{**}$ from $\mathbf{U}^*$
  - Advance H-part with $\mathbf{U}^{**}$ by $\Delta t/2$, to get the new solution $\mathbf{U}^{n+1}$
- The vertical part may be solved implicitly with DIRK (Diagonally Implicit Runge-Kutta) [9].
- For the implicit solver:
  - Inner linear solver uses Jacobian-Free GMRES **(Most expensive part)**.
  - It usually takes 1 or 2 iterations for the outer Newton solver.

[9] Durran, 2010

General IMEX

For the semi-implicit RK method

We define $f^{\text{im}}(\mathbf{U}(t),t) = \mathbf{L}^{\text{V}}(\mathbf{U}(t))$ and $f^{\text{ex}}(\mathbf{U}(t),t) = \mathbf{L}^{\text{H}}(\mathbf{U}(t))$.

$$\frac{d}{dt}\mathbf{U}_h = \mathbf{L}^{\text{H}}(\mathbf{U}_h) + \mathbf{L}^{\text{V}}(\mathbf{U}_h) \quad \text{in} \quad (t_n, t_{n+1}].$$

- Some popular choices of IMEX schemes,

$$\begin{array}{c|c} \mathbf{c}^{\text{ex}} & \mathbf{A}^{\text{ex}} \\ \hline & \mathbf{b}^T \end{array} \qquad \begin{array}{c|c} \mathbf{c}^{\text{im}} & \mathbf{A}^{\text{im}} \\ \hline & \mathbf{b}^T \end{array} .$$

Semi-implicit Runge-Kutta (IMEX2)
2-stage 2^{nd} order, $\alpha = 1 - \frac{1}{\sqrt{2}}$

$$\begin{array}{c|cc} 0 & 0 & \\ 1 & 1 & 0 \\ \hline & \frac{1}{2} & \frac{1}{2} \end{array} \qquad \begin{array}{c|cc} \alpha & \alpha & \\ 1-\alpha & 1-2\alpha & \alpha \\ \hline & \frac{1}{2} & \frac{1}{2} \end{array}$$

Third order IMEX (IMEX3, SIRK-3A)
(3-stage 3^{rd} order, $\alpha = \frac{5589}{6524} + \frac{75}{233}, \beta = \frac{7691}{26096} - \frac{26335}{78288} + \frac{65}{168}$)

$$\begin{array}{c|ccc} 0 & 0 & & \\ \frac{8}{7} & \frac{8}{7} & 0 & \\ \frac{120}{252} & \frac{71}{252} & \frac{49}{252} & 0 \\ \hline & \frac{1}{8} & \frac{1}{8} & \frac{3}{4} \end{array} \qquad \begin{array}{c|ccc} \frac{3}{4} & \frac{3}{4} & & \\ \alpha & \frac{5589}{6524} & \frac{75}{233} & \\ \beta & \frac{7691}{26096} & -\frac{26335}{78288} & \frac{65}{168} \\ \hline & \frac{1}{8} & \frac{1}{8} & \frac{3}{4} \end{array}$$

Outline

Inertia Gravity Wave[10]

Loading igw

Parameters

- Widely used for testing time-stepping methods in NH models
- Usually, $\Delta z \ll \Delta x$

[10] Skamarock & Klemp (1994)

Inertia Gravity Wave[10]

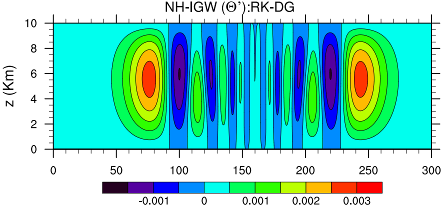

- $\Delta t = 0.04$ s for explicit RK-DG & $\Delta t = 0.4$ s for HEVI-DG
- $\Delta x = 500m$, $\Delta z = 50m$
- P^2-GL grid.

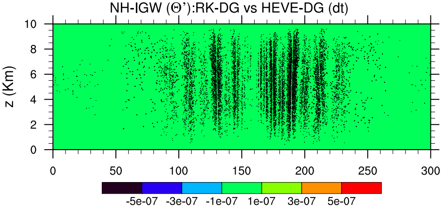

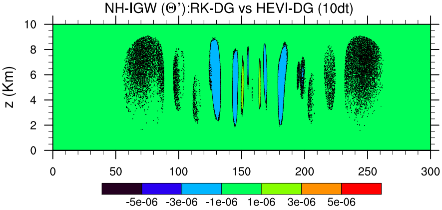

[10] Skamarock & Klemp (1994)

Inertia Gravity Wave Convergence Study

The Courant number for HEVI-DG is only constrained by horizontal grid-spacing (dx).

- $\Delta x = 10\Delta z$
- Δt for HEVI equals $10\Delta t$ for RK2.

h-convergence

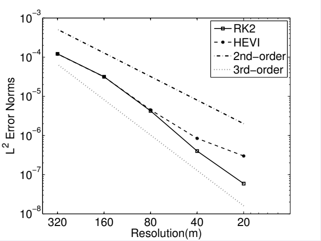

Horizontal Profile of θ'

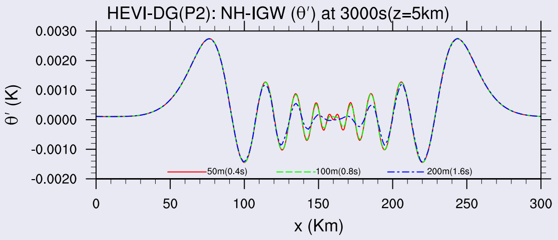

Straka Density Current[11]

- $\Delta t = 0.075$ s (both RK2 and HEVI), Diffusion Coeff $\nu = 75.0 m^2/s$. Handled by LDG.

Potential Thermal Temperature Perturbation

Loading Straka

[11] Straka et al. (1993)

Straka Density Current[11]

- Grid convergence: No noticeable changes in the fields at 100 m or higher resolutions

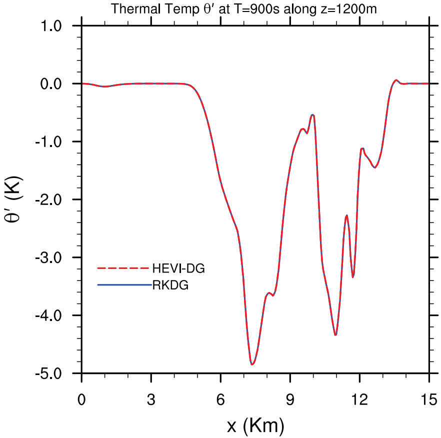

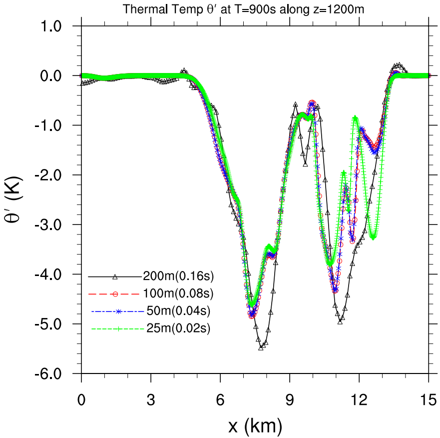

[11] Straka et al. (1993)

Linear Isolated Mountain [12]

Potential Thermal Temperature Perturbation

Loading ISM

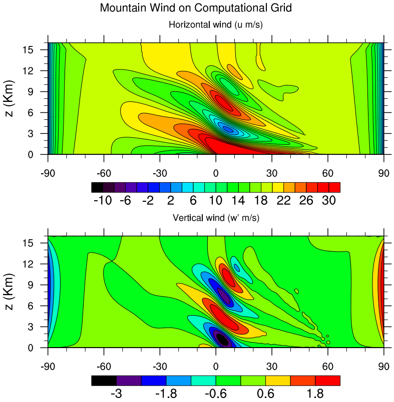

- $\Delta z \approx 222$ m, $\Delta x \approx 832$ m, $\Delta t = 0.15$ s (HEVI)

[12] Satoh (MWR, 2002)

Outline

Conclusion & Future Work

1. Moderate-order $(P^N, N = \{2,3,4\})$ DG-NH model performs well for benchmark test cases.
2. HEVI time-splitting effectively relaxes the CFL constraint to the horizontal dynamics only, and permits larger time-step.

Conclusion & Future Work

1. Moderate-order ($P^N, N = \{2, 3, 4\}$) DG-NH model performs well for benchmark test cases.
2. HEVI time-splitting effectively relaxes the CFL constraint to the horizontal dynamics only, and permits larger time-step.
3. Future work.
   - Incorporate HEVI in HOMME for full 3D DG-NH model
   - Improve the efficiency,for horizontal part: multi-rate time integration scheme, subcycling.
   - Adopt proper preconditioning process for efficient implicit solver in vertical part.
   - Test Hybrid DG for HEVI framework.(**Vertical Implicit Solver, Block Tri-diagonal Matrix, Reduce the degrees of freedom**)

Thank you!

Questions?

University of Colorado Boulder

NCAR

This work is supported by the DOE BER Program #DE-SC0006959